4-15-1997

Magnetism and morphology of Fe/Cu(111) films below two-dimensional percolation

J. Shen
Max–Planck–Institut für Mikrostrukturphysik, Weinberg 2, 06120 Halle, Germany, shenj5494@fudan.edu.cn

Ralph Skomski
University of Nebraska-Lincoln, rskomski2@unl.edu

M. Klaua
Max–Planck–Institut für Mikrostrukturphysik, Weinberg 2, 06120 Halle, Germany

H. Jenniches
Max–Planck–Institut für Mikrostrukturphysik, Weinberg 2, 06120 Halle, Germany

S. Sundar Manoharan
Max–Planck–Institut für Mikrostrukturphysik, Weinberg 2, 06120 Halle, Germany

See next page for additional authors

Magnetism and morphology of Fe/Cu(111) films below two-dimensional percolation

J. Shen, R. Skomski, M. Klaua, H. Jenniches, S. Sundar Manoharan, and J. Kirschner
Max–Planck–Institut für Mikrostrukturphysik, Weinberg 2, 06120 Halle, Germany

The magnetic properties of γ-iron films on Cu(111) below the two-dimensional percolation threshold of about 1.4 monolayer are investigated. Iron on flat Cu(111) surfaces forms triangular patches, while it forms stripes along step edges on vicinal surfaces. The films exhibit an easy magnetization axis perpendicular to the film plane and magnetic hysteresis at sufficiently low temperatures. The magnetization curves of the triangular iron patches are discussed in terms of Ising superparamagnetism. From Kerr hysteresis loops, we deduce that the first anisotropy constant K_1 in the superparamagnetic films is of order 0.345 ± 0.020 MJ/m^3. © *1997 American Institute of Physics.* [S0021-8979(97)45108-3]

I. INTRODUCTION

A key question in the magnetism of ultrathin films is what type of magnetic order exists at finite temperatures. Ferromagnetic order amounts to a nonzero spontaneous or zero-field equilibrium magnetization, whereas superparamagnets consist of blocks, characterized by a parallel spin orientation, but zero spontaneous magnetization. Due to thermal excitations, ferromagnetic long-range order may be destroyed even if the interatomic exchange coupling is ferromagnetic. A good example of thin-film superparamagnetism is the Langevin-like behavior of α-Fe deposited on MgO(001).[1]

In this article, we present morphological and magnetic studies on Fe/Cu(111) films below two-dimensional percolation. A key feature of our films is the existence of hysteresis below some temperature, which we discuss in terms of Ising superparamagnetism. Emphasis is put on the triangular iron patches; a detailed discussion of the magnetism of the stripes will be given elsewhere.

II. EXPERIMENTAL RESULTS

To study the magnetism of films below the two-dimensional percolation threshold, γ-Fe films were produced and investigated in an ultrahigh-vacuum system having a base pressure of 5×10^{-11} mbar. The system is equipped with facilities for scanning tunneling microscopy (STM), Auger electron spectroscopy, low-energy electron diffraction (LEED), and magneto-optical Kerr effect measurements (MOKE). The iron films were deposited on flat and vicinal Cu(111) surfaces from an iron wire heated by *e*-beam bombardment. During deposition, the substrate temperature was kept at 273 K in order to suppress copper diffusion.[2] STM and MOKE were used to study the morphology and the magnetism of the Fe/Cu(111) films, respectively.

Figure 1 shows typical STM topography images of nonpercolating iron films on (a) flat and (b) vicinal Cu(111) surfaces. The percolation threshold is about 1.4 monolayer (ML) for both types of surfaces. On flat surfaces, the iron atoms form more or less triangular patches, whereas the vicinal surfaces are dominated by iron stripes parallel to the steps. The stripes are located at the upper step edges of the terraces and aligned along the $\langle 011 \rangle$ direction, which is the

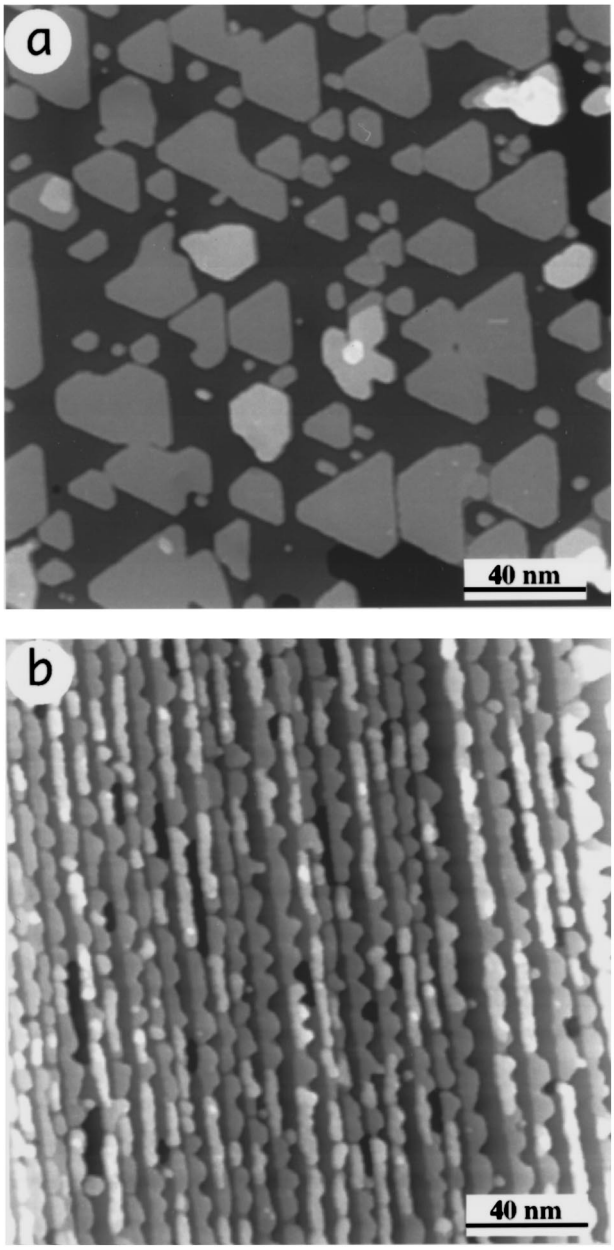

FIG. 1. STM morphology of ultrathin Fe/Cu(111) films below two-dimensional percolation: (a) a 1.1 ML film on a flat surface and (b) a 0.9 ML film on a vicinal surface for comparison.

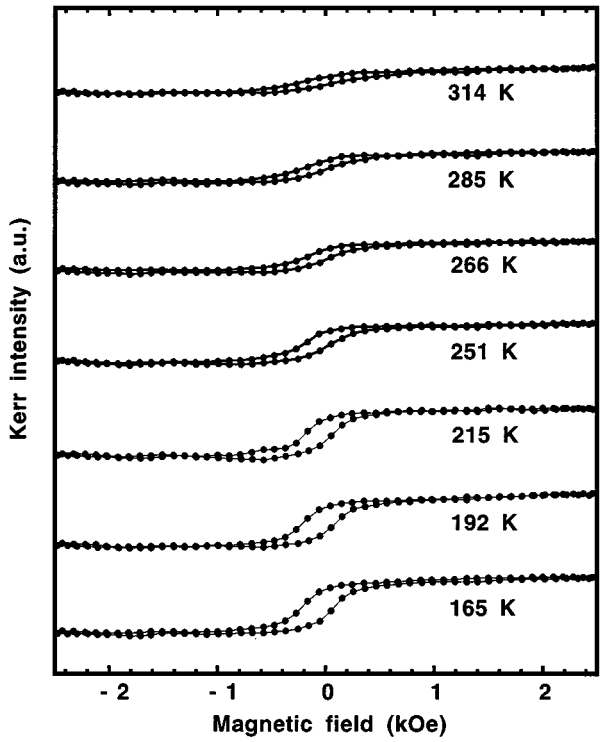

FIG. 2. (a) typical Kerr hysteresis loops for γ-Fe on Cu(111) below two-dimensional percolation: 1.1 ML on a flat surface. The parameter is the temperature at which the measurement was made. Note that the time to complete each loop is 40 s. (b) the hysteresis is time dependent: the time indicates a full loop cycle.

direction of the substrate steps. STM height measurements indicate that most iron patches have a thickness of two monolayers, whereas the stripes are monolayers ($\sim$70%) or double layers ($\sim$30%).

Below some thickness-dependent temperature, the iron patches and stripes exhibit magnetic hysteresis along the surface normal. The easy magnetization direction perpendicular to the film surface is inferred from the undetectably small magnetic signal in the longitudinal geometry. A typical series of hysteresis loops, measured on a 1.1 ML film on a flat Cu surface, is shown in Fig. 2(a). It is easy to see that remanence and coercivity decrease with increasing temperature. From the temperature dependence of the magnetization, we estimate that the critical temperature at which the saturation magnetization becomes zero is about 350 K. Furthermore, the hysteresis is time dependent. The two curves in Fig. 2(b) were measured at 190 K within 40 and 120 s, respectively. The difference between the two curves is a consequence of the activation process discussed in Sec. III C.

III. THEORETICAL ASPECTS

A. Langevin and Ising superparamagnetism

Let us now discuss the origin of the hysteresis in the magnetization curves of the iron patches (Fig. 2), which we tentatively ascribe to frozen or blocked Ising superparamagnetism. From the point of view of statistical mechanics, the difference between the classical Heisenberg and Ising models is the strength of the magnetocrystalline anisotropy. Since the ferromagnetic exchange inside each patch of volume V_0 is strong enough to assure a parallel spin alignment, it is sufficient to consider the Hamiltonian

$$H=-K_1V_0s_z^2-\mu_0M_0HV_0s_z. \tag{1}$$

Here the magnetization is given by $\mathbf{M}=M_0\mathbf{s}$, where $\mathbf{s}^2=1$ and M_0 is the spontaneous magnetization of the two-dimensional reference film. The equilibrium magnetization is now obtained from the partition function $Z=\int \exp(-H/k_BT)d\mathbf{s}$: $M=k_BT(\partial \ln Z/\partial H)/\mu_0V_0$.

For isolated atoms, K_1V_0/k_B does not exceed about 1 K, so that the anisotropy term in Eq. (1) can be neglected in the temperature range of interest. The magnetization is then given by the Heisenberg-type expression $M=M_sL(\mu_0M_sHV_0/k_BT)$, where $L(x)=\coth x-1/x$ is the Langevin function. In the present context, each iron patch consists of much more than 1000 exchange-coupled atoms, so that $K_1V_0\gg k_BT$. In this limit, the integral $\int ...d\mathbf{s}$ over all configurations having $\mathbf{s}^2=1$ reduces to an Ising sum over the two spin configurations $\mathbf{s}=\pm\mathbf{e}_z$, and the equilibrium magnetization is given by[3]

$$M=M_s\tanh\left(\frac{\mu_0M_sHV_0}{k_BT}\right). \tag{2}$$

This Ising character, which arises from the comparatively large cluster volume V_0, must not be confused with the Ising-type critical behavior of thin films,[4] which is related to long-range correlation in the vicinity of T_c.

At this point, it is worthwhile mentioning that Ising and Heisenberg magnetization curves differ only quantitatively and are difficult to distinguish from each other if factors such as volume distributions interfer. Note that the Heisenberg or Langevin character of the iron superparamagnets investigated in Ref. 1 is largely due to the presence of more than two easy magnetization directions.

B. Equilibrium magnetization curves

The equilibrium magnetism of γ-iron triangles, which form on flat surfaces, is given by Eq. (2). In principle, that equation could be used to fit the experimental magnetization curves, but Fig. 2 shows that hysteresis is not restricted to very low temperatures. Thus, to achieve a comprehensive description of the submonolayer films, it is necessary to include nonequilibrium effects (see Sec. III C).

In the case of vicinal surfaces, the interactions between different segments of a stripe have to be taken into account.[5] In this case, Eq. (2) valid for noninteracting Ising block spins has to be replaced by

$$\frac{M}{M_s}=\frac{\sinh\,(h/k_BT)}{\sqrt{\sinh^2\,(h/k_BT)+\exp(-4J/k_BT)}}, \tag{3}$$

where $h=\mu_0M_sHV_0$. In Eq. (3), which derives from the one-dimensional Ising model,[6] J is the exchange coupling between the segments. A detailed analysis of the interaction parameter J, which goes beyond the scope of this work, shows that $J<100$ K. This means that the segments are statistically more or less independent in the temperature range of interest.

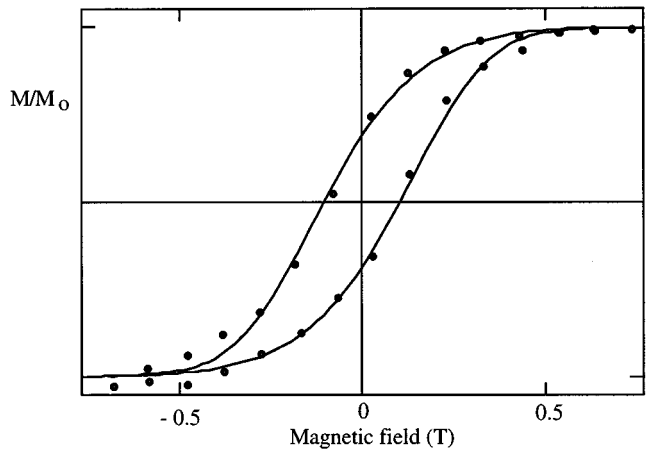

FIG. 3. Kerr and theoretical hysteresis loops of γ-iron on a 0.74 ML flat surface at 217 K. The deviations close to saturation are due to the size distribution of the patches.

C. Hysteresis

The starting point of the consideration of nonequilibrium superparamagnetism is the master equation[7]

$$\frac{dP(s_z)}{dt} = W(-s_z \rightarrow s_z)P(-s_z) - W(s_z \rightarrow -s_z)P(s_z), \tag{4}$$

where $P(s_z)$ and $W(-s_z \rightarrow s_z)$ denote probabilities and transition rates, respectively. Since the Ising model has no inherent dynamics, we choose

$$W(s_z \rightarrow -s_z) = \Gamma_0 \exp\left(-\frac{VK_1 + s_z \mu_0 HV}{k_B T}\right), \tag{5}$$

where the attempt frequency Γ_0 is of order 10^9–10^{12} s^{-1} (see e.g., Ref. 8) and K_1 matches the $s_z=0$ energy barrier appearing in Eq. (1).[9] This yields the differential equation of motion

$$\frac{dM}{dt} = \Gamma_0 \left(M_0 \sinh \frac{\mu_0 M_0 V_0 H}{k_B T} - M \cosh \frac{\mu_0 M_0 V_0 H}{k_B T} \right) \exp\left(-\frac{K_1 V_0}{k_B T}\right). \tag{6}$$

Figure 3 shows an experimental hysteresis loop fitted to Eq. (6) with $\mu_{\mathrm{Fe}}=0.75\ \mu_B$ (compare Ref. 10) and the sweeping rate $\mu_0 \partial H/\partial t = 0.01$ T/s. The parameters used to obtain the solid line in Fig. 3 are $K_1=0.345$ MJ/m^3 and $V_0=207$ nm^3. The fitting error bar for K_1 is about 0.020 MJ/m^3, but there might be some additional error due to the size distribution of the patches, which has not been taken into account.

Note that the blocking temperature corresponding to Eq. (6) is of order $K_1 V_0/k_B \ln(\Gamma_0 t_0)$, where t_0 is the time necessary to conduct the experiment. This equation determines the K_1 and V_0 window in which superparamagnetic blocking phenomena are visible.

IV. CONCLUSIONS

In conclusion, we have investigated the magnetism of Fe/Cu(111) films below the two-dimensional percolation threshold. Kerr magnetization curves of the triangular iron patches are presented and discussed in terms of Ising superparamagnetism. The present approach goes beyond earlier work in the sense that it is not restricted to equilibrium magnetization curves but also includes hysteresis loops fitted to the predictions of the superparamagnetic model.

[1] Y. Park, S. Adenwalla, G. P. Felcher, and S. D. Bader, Phys. Rev. B **52**, 12 779 (1995).
[2] M. Klaua, H. Höche, H. Jenniches, J. Barthel, and J. Kirschner (unpublished).
[3] L. Néel, Ann. Géophys. (Paris) **5**, 99 (1949).
[4] M. Bander and D. L. Mills, Phys. Rev. B **38**, 12 015 (1988).
[5] Even in the unlikely case that there are no morphological segments, thermal excitations will cause the stripes to decay into spin blocks of varying size.
[6] J. M. Yeomans, *Statistical Mechanics of Phase Transitions* (University Press, Oxford, 1992).
[7] K.-H. Fischer and A. J. Hertz, *Spin Glasses* (University Press, Cambridge, 1991).
[8] P. Gaunt, J. Appl. Phys. **59**, 4129 (1986).
[9] Other transition rates such as those of the Glauber model (see, e.g., Ref. 7) may be used equally well in the present context.
[10] U. Gradmann, W. Kümmerle, and P. Tilmans, Thin Solid Films **34**, 249 (1976).